ON THE ACCURACY OF PUSHBROOM AERIAL DIGITAL CAMERA

Qassim A. Abdullah, PhD, Chief Scientist
EarthData International, Inc.
Frederick, MD 21704
qabdullah@earthdata.com

ABSTRACT

With the rapid increase of aerial data acquisition using large-format digital aerial sensors during the last few years, there comes an urgent need to describe the geometrical accuracy of these sensors and their ability to obtain mapping accuracies according to different industry standards. This paper will deal with one kind of sensor, the pushbroom technology-based aerial sensor manufactured by Leica Geosystems. Results from 5 years of operation and several projects with map scales ranging from large (1:1,200) to medium (1:12,000) using the Leica ADS40 sensor, have demonstrated the capability of such sensors to capture highly accurate imagery suitable for the different map products just mentioned. The accuracy of the final derived products met the three major map accuracy standards, namely, the National Map Accuracy Standard (NMAS), the American Society of Photogrammetry and Remote Sensing (ASPRS), and the National Standard for Spatial Data Accuracy (NSSDA).

EVOLUTION OF THE METRIC DIGITAL CAMERA

During the ISPRS conference held in Vienna, Austria, during the year 2000, Leica Geosystems announced the sale of the first commercial large-format, aerial digital camera based on pushbroom technology. Shortly after, Z/I Imaging (presently Intergraph) announced the roll-out of their digital camera, the DMC, followed by Vexcel's UltraCAM D . All three large format sensors are suitable for standard photogrammetric work and can take the place of historically trusted metric aerial film cameras. Unlike the ADS40 sensor, both the DMC and the UltraCAM D are framing cameras with rectangular CCD array and, in principal, follow the same sensor model of the film cameras. On the other hand, the ADS40 sensor is based on a linear CCD array of 12,000 pixels and uses pushbroom techniques by which light passes through a linear slit before it is received by camera lens. Consecutive images from this linear CCD array are added together to form one long image that can extend hundreds of miles along the flight direction.

At the start, very few of the off-the-shelf software packages were able to handle data from a pushbroom sensor such as the ADS40. Since then, few more systems have developed the capability to import and process such data. The results presented here are all derived from products that were produced using the ADS40 sensor and processed by software called the "Pixel Factory" developed by Infoterra of France (formerly, ISTAR).

THEORETICAL ACCURACY OF ADS40/ISTAR DSM

In order to stand on the possible vertical accuracy from a digital sensor, the following formula is modified to suit the digital imagery:

$$\mathbf{S_z = \sqrt{((H/B * a_2 * GSD)^2 + S_{(orientation)}^2)}} \quad \ldots\ldots\ldots\ldots\ldots\ldots\ldots\ldots\ (1)$$

where,

$\mathbf{S_z}$ is the error in elevation;
H is the flying height;
B is the stereo base;
$\mathbf{a_2}$ is a coefficient that depends on B/H ratio, smaller for large B/H and larger for smaller B/H;
$\mathbf{S_{(orientation)}}$ is the standard error of the effect of sensor orientation on the ground, assuming that the IMU orientations after refined with the process of serial triangulation is accurate to 10 arc seconds in the three rotation angles, omega, phi, and kappa.

As the different look-angle combinations result in different B/H ration, then one expects that there are some quality differences in the different stereo parallactic angles resulting from the different look angle combinations, as presented in Table I. Substituting the values of B/H ration of Table I into equation (1), it is possible to obtain the theoretical accuracy values for the different flying heights and stereo angles combination of the ADS40 as illustrated in Table II and Appendix I.

Table I. Look angles and resulting parallactic angles for ADS40

Stereo-pair combination	Resulting parallactic angle (degree)	Bands combination description
ND-PANF28	28	Nadir and B&W forward at 28 degree
ND-PANB14	14	Nadir and B&W backward at 14 degree
PANB14-PANF28	42	Backward at 14 degree and B&W forward at 28 degree
ND-GRNF16	16	Nadir and green forward at 16 degree
PANB14-GRNF16	30	Backward at 14 degree and green forward at 16 degree

Table II Calculation of Theoretical Vertical Accuracy for ADS40 Elevation Models

Flying Height (m)	Resulting GSD (m)	Average Theoretical Vertical Accuracy Sz (RMSE) (m)	Contour Interval Suitability (m)	Contour Interval Suitability (ft)
1,440	0.15	0.14	0.60	2
2,881	0.30	0.29	1.2 to 1.5	4 to 5
5,761	0.60	0.58	2.40 to 3.0	8 to 10
9,602	1.00	0.96	4.50	15

The accuracy figures in Table II can only be achieved if all or part of the DTM is obtained from stereocompilation and the project has enough accurately surveyed ground control points. Autocorrelation techniques are disregarded here mainly due to the poor differentiation between the bare-earth elevation model that is necessary to extract contour-quality elevation data and the elevations of tress and manmade objects associated with autocorrelated elevation models.

ACHIEVED ACCURACY FROM ADS40/ISTAR DATA PROCESSING

In order to validate the vertical accuracy of the elevation data derived in equation 1 from an ADS40 data produced through an ISTAR workflow, several large projects were analyzed with the results compared to that of equation one.

As for the horizontal accuracy, past experience with multiple projects demonstrated the geometrical strength of the planimetric coordinates, therefore, less emphasis was directed to the horizontal accuracy modeling and no model was developed for the theoretical horizontal accuracy. However, actual results of the horizontal accuracy for several projects were presented in later sections.

Data Processing

After processing the IMU/GPS data, the orientation of every scan line is computed and stored with the raw imagery. Each block consists of multiple flight lines, each of which is tied to the adjacent line(s) through the process of tie-point collection during the aerial triangulation process

Aerial triangulation was performed on all the discussed projects in order to refine the GPS/IMU-derived sensor position and orientation and to make it more suitable for producing high fidelity engineering-scale maps and products. The amount of ground control points used in the aerial triangulation solution and for verifying the aerial triangulation results varied according to the scale, shape, and size of the project, as well as the intended accuracy.

Imagery collected with a pushbroom sensor such as the ADS40 posses a unique characteristic as it is in the form of one long image that can extend to hundreds of miles, see figure 1. However, this long image can also be looked at as slivers of images with a dimension of 1 pixel high by 12,000 pixels wide or the width of the linear array. This later image is mathematically modeled to resemble the conventional frame of the film or area array digital camera; with an orthogonal image coordinate system, the x-axis is along the flight direction and the y-axis is along the line connecting between the two wings of the aircraft (see figure 2).

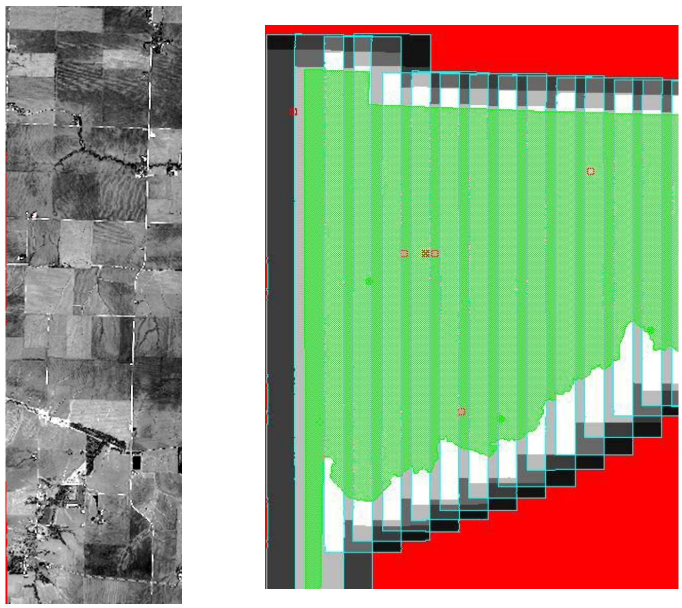

a b

Figure 1. (a) Image of ADS40 flight line coverage; (b) Foot prints of multi flight lines block.

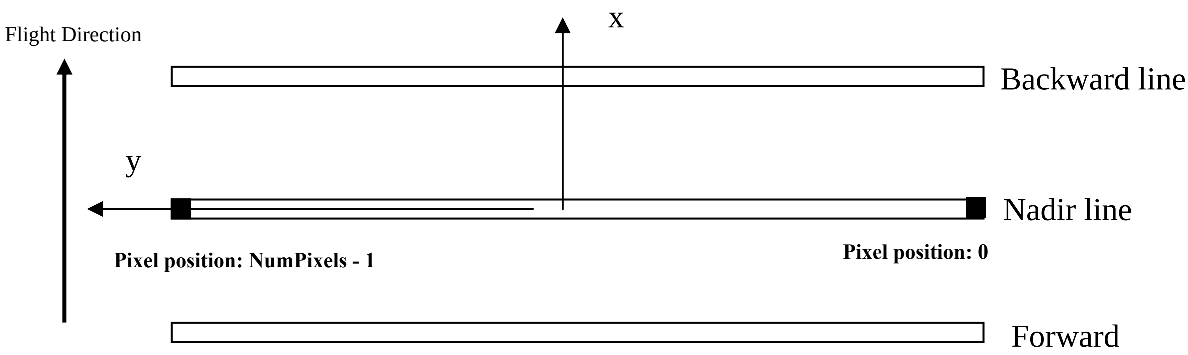

Figure 2. Image coordinates system for ADS40 in the focal plane.

During the aerial triangulation process, a set of tie-points is generated between the adjacent flightlines as it is the case in conventional aerial triangulation. However, there are no pass points in the sense of the pass points for the framing camera as the there is just one long image along the project boundary.

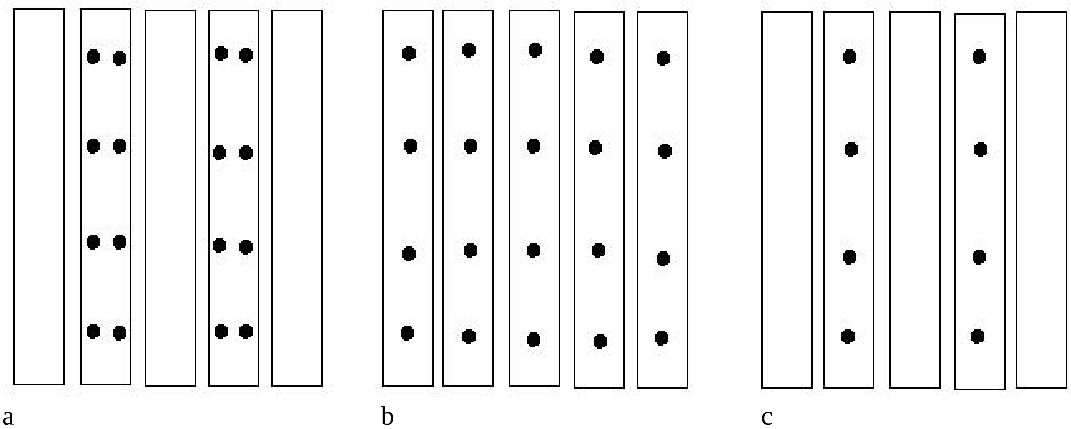

Figure 3. Tie-points selection for (a) 30%, (b) 60%, and (c) 80% Side lap.

THE MATHEMATICAL MODEL

The essence of refining or determining the geometrical model for ADS40 imagery during the aerial triangulation process is based on the adjustment of the following parameters for an entire flight: (1) Three angles representing the bias in relative orientation of the IMU and the camera focal plane. These angles account for the mechanical distortions over a thermal cycle of use of the camera. Typical angles changes are in the magnitude of 100 micro radian (20 arc seconds) or less. (2) Three translation parameters accounting for the inaccuracy or biases of the absolute position given by the GPS. Such bias is typically less than 50 cm in each of the E, N, and height directions.

Several additional parameters can be adjusted in the bundle block solution of the mathematical model utilized by ISTAR software if necessary. The position biases of the camera in the IMU coordinates system, biases and drifts in the position and orientation of the IMU in WGS84 geocentric system, and camera focal length and geometric stability of the focal plane (i.e. CCD array deformation) represent some of these parameters.

ACCURACY EVALUATION

According to the three map standards, the vertical and horizontal accuracy for the three scales used for the study are given in Table III:

Table III. Vertical and horizontal map accuracy according to NMAS, ASPRS, and NSSDA map standards

Map Standard	Data Type	Map Scale		
		1:1,200 or 0.15 m GSD (m)	1:2,400 or 0.30 m GSD (m)	1:4,800 or 0.60 m GSD (m)
NMAS at 90%	Horizontal	1.00	2.00	4.00
	Vertical	0.30	0.76	1.50
ASPRS at 68% (RMSE)	Horizontal	0.30	0.60	1.20
	Vertical	0.20	0.50	1.00
NSSDA at 95%	Horizontal	0.50	1.00	2.10
	Vertical	0.40	0.80	1.60

Accuracy during different stages of production was evaluated for 29 projects that were flown with the ADS40 sensor. The first stage is during aerial triangulation phase during which the root mean squares error (RMSE) of the residual of fitting the surveyed ground control points coordinates to the one obtained from the simultaneous bundle block adjustment solution as the resulting statistics which is measured by. Here it should be mentioned that the aerial triangulation is evaluated to a different and more stringent standard. As an acceptance measure that we set for our internal operation, an RMSE of 1/10,000 of the flying height or better must be met before the aerial triangulation results are accepted and finalized.

After the aerial triangulation accuracy is achieved, stereo-pairs were generated and imported into Intergraph Image Station to verify the accuracy of the stereo-pairs. During the later process, all the available ground control and check points were visited in stereo mode and the measured Easting, Northing, and Elevation were tabulated. Here, the results were evaluated according to the common map accuracy standards such as NMAS, ASPRS, and NSSDA. This step is essential to stand on the accuracy of the compiled maps for the project based on the accepted aerial triangulation solution. The accuracy of the stereo pairs should be somewhere between AT and map accuracy as it has minimal errors budget as compared to the ortho production, for example in which the terrain elevation data can contribute to the final map accuracy figures.

Finally, the last stage of the accuracy verification is the one obtained from the produced rectified imagery. This also should meet the three map accuracy standards utilized for this study. Tables IV through VI list the vertical and horizontal accuracy obtained from ADS40 for different mapping scales for different products.

Table IV. Accuracy for 1:1,200 or GSD=15 cm projects

Project Info		**Stereo Pairs Results RMSE (m)**			**AT Results RMSE (m)**			**Ortho Results RMSE (m)**	
Project ID	GSD (m)	Easting	Northing	Elevation	Easting	Northing	Elevation	Easting	Northing
Project 1	0.15	0.17	0.09	0.12	0.12	0.14	0.06	0.07	0.16
Project 2	0.15	0.13	N/A	0.24	0.03	0.08	0.14	0.09	0.06
Project 3	0.15	0.17	0.18	0.14	0.06	0.11	0.13	N/A	N/A
Project 4	0.15	0.1	0.1	0.13	0.10	0.06	0.13	0.12	0.15
Project 5	0.15	N/A	N/A	N/A	0.06	0.09	0.09	0.09	0.23
Project 6	0.15	N/A	N/A	N/A	0.14	0.11	0.15	0.19	0.16
Project 7	0.15	0.14	0.29	0.18	0.06	0.05	0.18	0.09	0.11
Number of Projects		5	5	5	7	7	7	6	6
RMSE (m)		**0.14**	**0.18**	**0.17**	**0.09**	**0.10**	**0.13**	**0.12**	**0.15**

Table V. Accuracy for 1:2,400 or GSD=30 cm projects

Project Info		**Stereo Pairs Results RMSE (m)**			**AT Results RMSE (m)**			**Ortho Results RMSE (m)**	
Project ID	GSD (m)	Easting	Northing	Elevation	Easting	Northing	Elevation	Easting	Northing
Project 8	0.3	0.22	0.17	0.02	0.10	0.12	0.10	0.18	0.10
Project 9	0.3	0.01	0.27	0.365	0.13	0.11	0.12	0.18	0.17
Project 10	0.3	0.13	0.14	0.34	0.07	0.06	0.09	0.20	0.16
Project 11	0.3	0.23	0.17	0.27	0.05	0.08	0.10	0.09	0.15
Project 12	0.3	0.15	0.21	0.18	N/A	N/A	N/A	N/A	N/A
Project 13	0.3	0.00	0.05	0.26	0.08	0.06	0.07	N/A	N/A
Project 14	0.3	0.34	0.3	0.39	0.18	0.18	0.26	0.29	0.30
Project 15	0.3	0.31	0.3	0.27	0.15	0.16	0.14	0.28	0.18
Project 16	0.3	0.14	0.15	0.15	0.11	0.10	0.10	0.20	0.12
Project 17	0.3	0.27	0.16	0.29	0.07	0.08	0.09	0.21	N/A
Project 18	0.3	0.48	0.22	0.14	0.04	0.05	0.05	0.36	0.11
Project 19	0.3	0.08	0.16	0.29	0.12	0.15	0.13	0.49	0.22
Project 20	0.3	0.19	0.3	0.26	0.17	0.07	0.04	N/A	N/A
Project 21	0.3	0.11	0.12	0.15	0.10	0.11	0.10	0.37	0.26
Project 22	0.3	0.18	0.26	0.05	0.11	0.11	0.09	0.07	0.06
Project 23	0.3	0.1	0.28	0.23	0.06	0.08	0.10	0.13	0.18
Project 24	0.3	0.38	0.30	0.19	0.12	0.12	0.09	0.10	0.13

Project Info		Stereo Pairs Results			AT Results			Ortho Results	
		RMSE (m)			RMSE (m)			RMSE (m)	
Project ID	GSD (m)	Easting	Northing	Elevation	Easting	Northing	Elevation	Easting	Northing
Number of Projects		17	17	17	16	16	16	14	14
RMSE (m)		**0.23**	**0.22**	**0.25**	**0.11**	**0.11**	**0.11**	**0.25**	**0.19**

Table VI. Accuracy for 1:4,800 or GSD=60 cm projects

Project Info		Stereo-pairs Results			AT Results			Ortho Results	
		RMSE (m)			RMSE (m)			RMSE (m)	
Project ID	GSD (m)	Easting	Northing	Elevation	Easting	Northing	Elevation	Easting	Northing
Project 25	0.6	0.26	0.23	0.32	0.07	0.06	0.03	0.17	0.15
Project 26	0.6	N/A	N/A	N/A	0.24	0.21	0.18	0.79	0.56
Project 27	0.6	N/A	N/A	N/A	0.01	0.15	0.28	0.11	0.19
Project 28	0.6	0.22	0.17	0.36	0.04	0.12	0.12	0.82	0.55
Project 29	0.6	0.18	0.23	0.32	N/A	N/A	N/A	N/A	N/A
Number of Projects		3	3	3	4	4	4	4	4
RMSE (m)		**0.22**	**0.21**	**0.33**	**0.13**	**0.15**	**0.18**	**0.58**	**0.41**

Accuracy of Stereo Pairs

From the accuracy figures presented in tables IV, we can conclude that for projects 1 to 7, the horizontal accuracy of RMSE < 30 cm is well within the required map accuracy according to the three map accuracy standards NMAS, ASPRS, and NSSDA for map scale of 1:1,200 or 1”=100’. The same conclusion can be drawn from the results of projects 8 to 24 of table V as it met the accuracy requirements for map scale of 1:2,400 or 1”=200’ for the three standards. In addition, the results from projects 25 and 29, which well met the accuracy requirements for mapping scale of 1:4,800 or 1”=400’ according to the three map standards.

As for the achieved vertical accuracy, figures for projects 1-7 met the vertical accuracy requirement for the 0.60 meter or 2 ft contour interval that is expected from the scale of the imagery with GSD of 0.15 meter according to all the three map standards. The same conclusion applies to projects 8-24 as the vertical accuracy met the accuracy requirements for the 1.5 meter of 5’ contour interval that is expected from a map scale of 1:2,400 or 1”=200’. The results from projects 25 to 29 shows that all projects met the vertical accuracy requirements for the generation of 3.0 meter or 10 ft contour interval expected from map products with scale of 1:4,800 or 1”=400 ft.

It is interesting to find out that the accuracy obtained from map scale of 1:1,200 is almost the same as the one obtained from scale 1:2,400 despite the fact that the photography of the later was flown from twice the altitude as the one for the 1:2,400. The only logical explanation for this observation is that the ADS40/ISTAR solution relies heavily on the GPS/IMU-derived orientation and since the accuracy of the airborne GPS is believe to be within 10 cm at best, then the effect of the airborne GPS/IMU error budget on the lower altitude imagery is greatly exaggerated. The expected errors in the airborne GPS/IMU is not linearly proportional to the flying altitude, therefore the accuracy expected from a scale of 1:2,400 is not necessary expected to be half the accuracy obtained from the 1:1,200 scale as it is obvious from tables IV and V.

Accuracy of Aerial-triangulation

The accuracy obtained from the process of aerial triangulation is expected to exceed the one from stereo pairs or orthoimagery and which is targeted to meet 1/10,000 of the flying height. For projects with 1:1,200 map scale, and RMSE of 0.09, 0.10, and 0.13 meter were achieved for the three coordinates E, N, and elevation respectively. As the imagery were flown from an altitude of 1,440.0 meter or 4,725.0’ (projects given in table IV), the aerial triangulation acceptance criteria was set to be 0.14 meter or 0.47’ for the three different coordinates. Therefore, the aerial triangulation criterion of 1/10,000 of the flying height was always met for all the projects with GSD of 0.15 meter or 0.50 ft.

As for projects 8-24, which were flown from an altitude of 2,880.0 meter or 9,448.0 ft and resulted in aerial triangulation acceptance criteria of 0.29 meter or 0.95 ft, all projects were well within the acceptance criteria as it is clear from table V. Same conclusion is obtained for projects 25 to 29 that were flown from an altitude of 5,760.0 meter or 18,897.0 ft or aerial triangulation acceptance criteria of 0.58 meter or 1.89 ft as it is given in table VI.

One should pay attention to the vertical theoretical accuracy figures that were given in table II and how these relate to the actual results listed in tables IV through VI under the aerial triangulation and stereo pairs columns. Despite the fact that some of the assumptions made in equation (1) can be looked at as subjective, as people may disagree on the practical value used for the coefficient a2, the practical results came reasonably within the predicted vertical accuracy. In addition, looking into figures 4 through 6, only can easily notice the error propagation throughout the different production stages of the mapping products. While the accuracy of aerial triangulation exceeded that for both stereo-pairs readings and ortho imagery, the accuracy of the later two stays close to each other as one should expect. This is clearly, because ortho production for example uses additional processes and materials that can add to the error budget of aerial triangulation such as the digital elevation model used in the ortho rectification process.

Accuracy of Ortho Imagery

The final stage of accuracy assessment is performed on the generated orthophoto map. The results from all 29 projects analyzed in this paper, which is given in tables IV through VI, were found to be within the threshold of the three map accuracy standards that were given in table III.

The resultant ortho accuracy is of special importance as the orthophoto products dominate the mapping market. It is interesting to see in tables IV through VI that most the projects with GSD of 0.30 meter or map scale of 1:2,400 (or 1”=200’) are found to meet the requirements for the horizontal accuracy standard for map scale of 1:1,200 (or 1”=100’). Results like the ones obtained in this research may force future amendments to the thresholds of the accuracy used in different map standards.

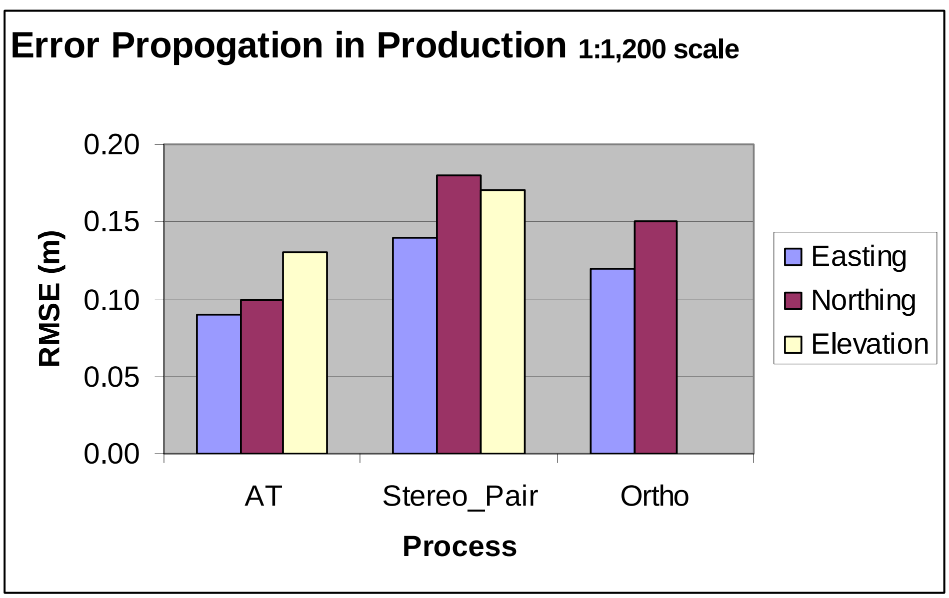

Figure 4. Error Propagation from Aerial triangulation through Ortho Production Scale 1:1,200.

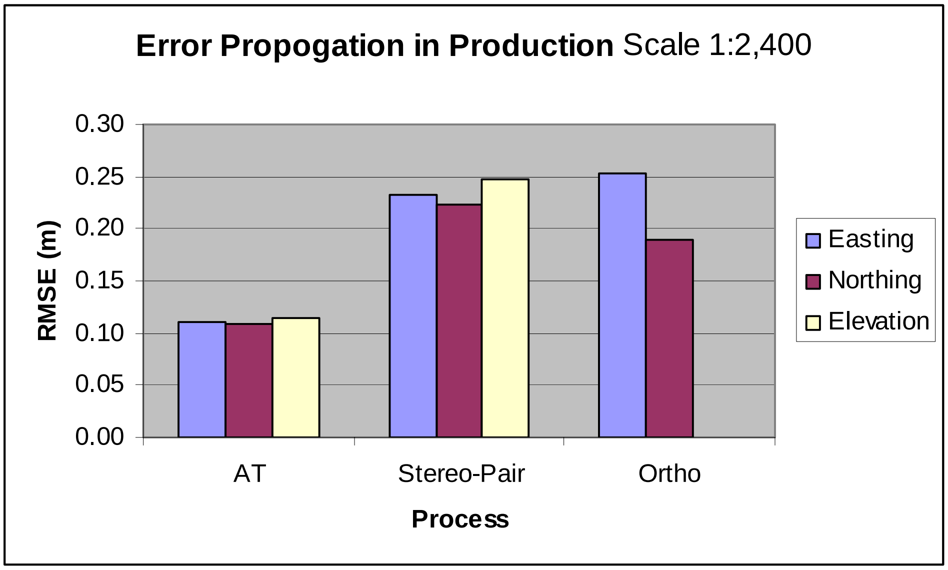

Figure 5. Error Propagation from Aerial triangulation through Ortho Production Scale 1:2,400.

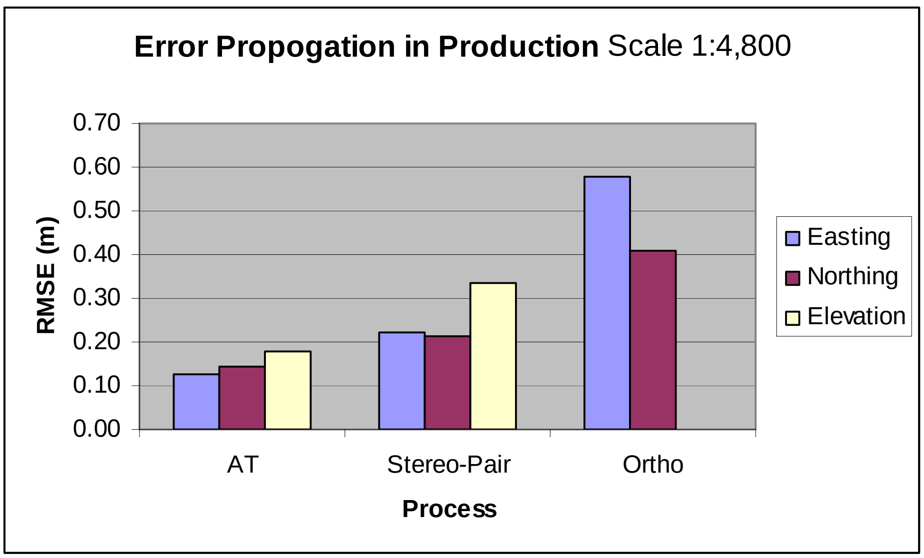

Figure 6. Error Propagation from Aerial triangulation through Ortho Production Scale 1:4,8 00.

CONCLUSIONS

There has been very few accuracy results presented since large-format digital aerial sensors were introduced to the mapping industry. According to the author's experience with the ADS40 pushbroom sensor from Leica Geosystems for the last 5 years, the new digital sensor technology is proven to possess high geometric quality, as required for metric mapping cameras. It is found that the theoretical prediction for the vertical accuracy of the sensor is in agreement with the actual results from 29 projects. The resultant map accuracy produced from such sensors is continuously found to be of better standing than the maps produced from film cameras with the same scale which may require special attention and a call to look into new acceptance criteria for map accuracy at different map accuracy standards.

APPENDIX I
THEORETICAL VERTICAL ACCURACY COMPUTATION FROM ADS40 DIGITAL SENSOR

Flying Height (m)	Resulting GSD (m)	Average Theoritical Vertical Accuracy Sz (RMSE) meter	**ND-PANF28** (28 degrees)			**ND-PANB14** (14 degrees)			**PANB14-PANF28** (42 degrees)			**ND-GRNF16** (16 degrees)			**PANB14-GRNF16** (30 degrees)			Average vertical accuracy (m)
			Stereo Base (m)	B/H	Sz	Stereo Base (m)	B/H	Sz	Stereo Base (m)	B/H	Sz	Stereo Base (m)	B/H	Sz	Stereo Base (m)	B/H	Sz	
720	**0.075**	0.07	383	0.5	0.07	180	0.2	0.08	648	0.9	0.05	206	0.3	0.08	416	0.6	0.07	0.07
960	0.100	0.10	511	0.5	0.10	239	0.2	0.11	865	0.9	0.06	275	0.3	0.11	554	0.6	0.10	0.10
1,440	0.150	**0.14**	766	0.5	0.15	359	0.2	0.17	1,297	0.9	0.09	413	0.3	0.17	832	0.6	0.15	0.14
1,920	0.200	0.19	1,021	0.5	0.19	479	0.2	0.22	1,729	0.9	0.12	551	0.3	0.22	1,109	0.6	0.19	0.19
2,401	0.250	0.24	1,276	0.5	0.24	599	0.2	0.28	2,161	0.9	0.16	688	0.3	0.28	1,386	0.6	0.24	0.24
2,881	0.300	**0.29**	1,532	0.5	0.29	718	0.2	0.33	2,594	0.9	0.19	826	0.3	0.33	1,663	0.6	0.29	0.29
3,361	0.350	0.34	1,787	0.5	0.34	838	0.2	0.39	3,026	0.9	0.22	964	0.3	0.39	1,940	0.6	0.34	0.34
3,841	0.400	0.38	2,042	0.5	0.39	958	0.2	0.45	3,458	0.9	0.25	1,101	0.3	0.45	2,217	0.6	0.39	0.38
4,321	0.450	0.43	2,297	0.5	0.44	1,077	0.2	0.50	3,891	0.9	0.28	1,239	0.3	0.50	2,495	0.6	0.44	0.43
4,801	0.500	0.48	2,553	0.5	0.49	1,197	0.2	0.56	4,323	0.9	0.31	1,377	0.3	0.56	2,772	0.6	0.49	0.48
5,281	0.550	0.53	2,808	0.5	0.53	1,317	0.2	0.61	4,755	0.9	0.34	1,514	0.3	0.61	3,049	0.6	0.53	0.53
5,761	0.600	**0.58**	3,063	0.5	0.58	1,436	0.2	0.67	5,187	0.9	0.37	1,652	0.3	0.67	3,326	0.6	0.58	0.58
6,241	0.650	0.62	3,319	0.5	0.63	1,556	0.2	0.72	5,620	0.9	0.40	1,790	0.3	0.72	3,603	0.6	0.63	0.62
6,721	0.700	0.67	3,574	0.5	0.68	1,676	0.2	0.78	6,052	0.9	0.43	1,927	0.3	0.78	3,881	0.6	0.68	0.67
7,202	0.750	0.72	3,829	0.5	0.73	1,796	0.2	0.83	6,484	0.9	0.47	2,065	0.3	0.83	4,158	0.6	0.73	0.72
7,682	0.800	0.77	4,084	0.5	0.78	1,915	0.2	0.89	6,917	0.9	0.50	2,203	0.3	0.89	4,435	0.6	0.78	0.77
8,162	0.850	0.81	4,340	0.5	0.83	2,035	0.2	0.95	7,349	0.9	0.53	2,340	0.3	0.95	4,712	0.6	0.83	0.81
8,642	0.900	0.86	4,595	0.5	0.88	2,155	0.2	1.00	7,781	0.9	0.56	2,478	0.3	1.00	4,989	0.6	0.88	0.86
9,122	0.950	0.91	4,850	0.5	0.92	2,274	0.2	1.06	8,213	0.9	0.59	2,616	0.3	1.06	5,267	0.6	0.92	0.91
9,602	1.000	**0.96**	5,105	0.5	0.97	2,394	0.2	1.11	8,646	0.9	0.62	2,753	0.3	1.11	5,544	0.6	0.97	0.96
11,000	2.000	1.81	5,849	0.5	1.85	2,743	0.2	2.14	9,904	0.9	1.09	3,154	0.3	2.14	6,351	0.6	1.85	1.81